The landscape of metabolic pathway dependencies in cancer cell lines

James H. Joly[1], Brandon T.L. Chew[1,#], and Nicholas A. Graham[1,2,3]

[1]Mork Family Department of Chemical Engineering and Materials Science,

[2]Norris Comprehensive Cancer Center, University of Southern California

[3]Leonard Davis School of Gerontology,

University of Southern California, Los Angeles, CA 90089

[#]Present address: Department of Pharmaceutical Sciences and Pharmacogenomics, University of California, San Francisco

Running title:

Metabolic pathway dependencies in cancer

To whom correspondence should be addressed: Nicholas A. Graham, University of Southern California, Los Angeles, 3710 McClintock Ave., RTH 509, Los Angeles, CA 90089. Phone: 213-240-0449; E-mail: nagraham@usc.edu

Abstract

The metabolic reprogramming of cancer cells creates metabolic vulnerabilities that can be therapeutically targeted. However, our understanding of metabolic dependencies and the pathway crosstalk that creates these vulnerabilities in cancer cells remains incomplete. Here, by integrating gene expression data with genetic loss-of-function and pharmacological screening data from hundreds of cancer cell lines, we identified metabolic vulnerabilities at the level of pathways rather than individual genes. This approach revealed that metabolic pathway dependencies are highly context-specific such cancer cells are vulnerable to inhibition of one metabolic pathway only when activity of another metabolic pathway is altered. Notably, we also found that the no single metabolic pathway was universally essential, suggesting that cancer cells are not invariably dependent on any metabolic pathway. In addition, we confirmed that cell culture medium is a major confounding factor for the analysis of metabolic pathway vulnerabilities. Nevertheless, we found robust associations between metabolic pathway activity and sensitivity to clinically approved drugs that were independent of cell culture medium. Lastly, we used parallel integration of pharmacological and genetic dependency data to confidently identify metabolic pathway vulnerabilities. Taken together, this study serves as a comprehensive characterization of the landscape of metabolic pathway vulnerabilities in cancer cell lines.

Introduction

The reprogramming of cellular metabolism was one of the earliest discovered hallmarks of cancer (Warburg, 1956). Cancer cells rewire their metabolism to satisfy the bioenergetic, biosynthetic, and redox demands of tumors. In turn, these metabolic adaptations create cancer-specific vulnerabilities that can be therapeutically targeted (Luengo et al., 2017). Much research has focused on how individual mutations or DNA copy number alterations reprogram tumor metabolism and create therapeutic opportunities (Dang et al., 2009; Graham et al., 2017; Maddocks et al., 2013; Muller et al., 2012; Sharma et al., 2016; Ward et al., 2010; Zhang et al., 2020). However, given that metabolic pathways consist of multiple enzymes which collectively regulate metabolic flux, studying the effects of individual genes may not reflect cancer cell metabolic vulnerabilities at the pathway level. As a result, our understanding of cancer cell dependency on metabolic pathways remains incomplete.

Recent developments in large scale CRISPR-based genetic (Meyers et al., 2017; Tsherniak et al., 2017) and pharmacologic screening (Corsello et al., 2020) along with large panels of comprehensively characterized cancer cell lines (Ghandi et al., 2019) have proved powerful tools for identification of genes essential for cancer cell survival (Lagziel et al., 2019), elucidation of drug mechanism-of-action (Gonçalves et al., 2020; Lin et al., 2019; Meyers et al., 2017), and discovery of novel candidate drug targets (Barretina et al., 2012; Garnett et al., 2012). Furthermore, parallel integration of both pharmacologic and gene loss-of-function data has been used to identify drug mechanism(s) of action (Deans et al., 2016; Lin et al., 2019; Subramanian et al., 2017; Wang et al., 2017). While these databases have served as a rich resource to explore individual gene vulnerabilities and drug sensitivities, there exists a need to probe these datasets on the pathway level.

Here, we aimed to identify cancer cell dependencies on metabolic pathways rather than individual metabolic genes. To do so, we used gene expression data from the Cancer Cell Line Encyclopedia (CCLE) to infer metabolic pathway activity and then integrated these pathway activities with data from genetic and pharmacologic screens across hundreds of cell lines. We show that this approach provides a comprehensive characterization of the landscape of metabolic pathway dependencies in cancer cell lines. In addition to demonstrating the context-specific nature of metabolic pathway dependence, we identified both known and novel metabolic vulnerabilities, discovered robust associations between drug response and metabolic pathway activity, and independently found metabolic pathway essentialities in both genetic and pharmacological screens. Collectively, we present an approach to integrate gene expression, gene dependency, and drug response data to identify cancer cell dependencies on metabolic pathways.

Results

Genetic Pathway Dependency Enrichment Analysis Identifies Metabolic Pathway Dependencies in Genetic Screens

To identify metabolic pathway dependencies, we analyzed gene expression data and CRISPR-Cas9 loss-of-function screens from 689 cancer cell lines overlapping between the Cancer Cell Line Encyclopedia (CCLE) (Barretina et al., 2012; Ghandi et al., 2019) and the Cancer Dependency Map (Tsherniak et al., 2017). First, we inferred metabolic pathway activity for each cell line using single-sample gene set enrichment analysis (ssGSEA) of the RNAseq data from each cell line (Barbie et al., 2009). To focus on metabolism, we queried 69 metabolic pathways from the Kyoto Encyclopedia of Genes and Genomes (KEGG) (Kanehisa et al., 2014). Because metabolism is influenced by culture type (Li et al., 2019) and culture medium (Lagziel et al., 2019), we first divided cancer cell lines by culture type (e.g., adherent v. suspension culture) and media (e.g., RPMI v. DMEM) (**Fig. 1A**). Cell lines without annotations for either of these features were removed, leaving 300 adherent cell lines cultured in RPMI, 153 adherent cell lines cultured in DMEM, 66 suspension cell lines cultured in RPMI, and 2 suspension cell lines cultured in DMEM. Since the number of suspension cell lines was small, we focused our analysis on adherent cell lines. The resulting ssGSEA normalized enrichment scores (NESs) represent the metabolic pathway activity relative to all other cell lines within the respective cell culture medium. Next, we correlated the cell line-specific NESs for each metabolic pathway with cell fitness effects from CRISPR-Cas9 loss-of-function screens (16,643 gene knockouts). Here, each correlation coefficient represents the association between metabolic pathway activity and gene essentiality, with positive values representing increased gene dependency in cell lines with increased metabolic pathway activity. Conversely, a negative correlation indicates increased gene dependency in cell lines with decreased metabolic pathway activity. Finally, to measure the

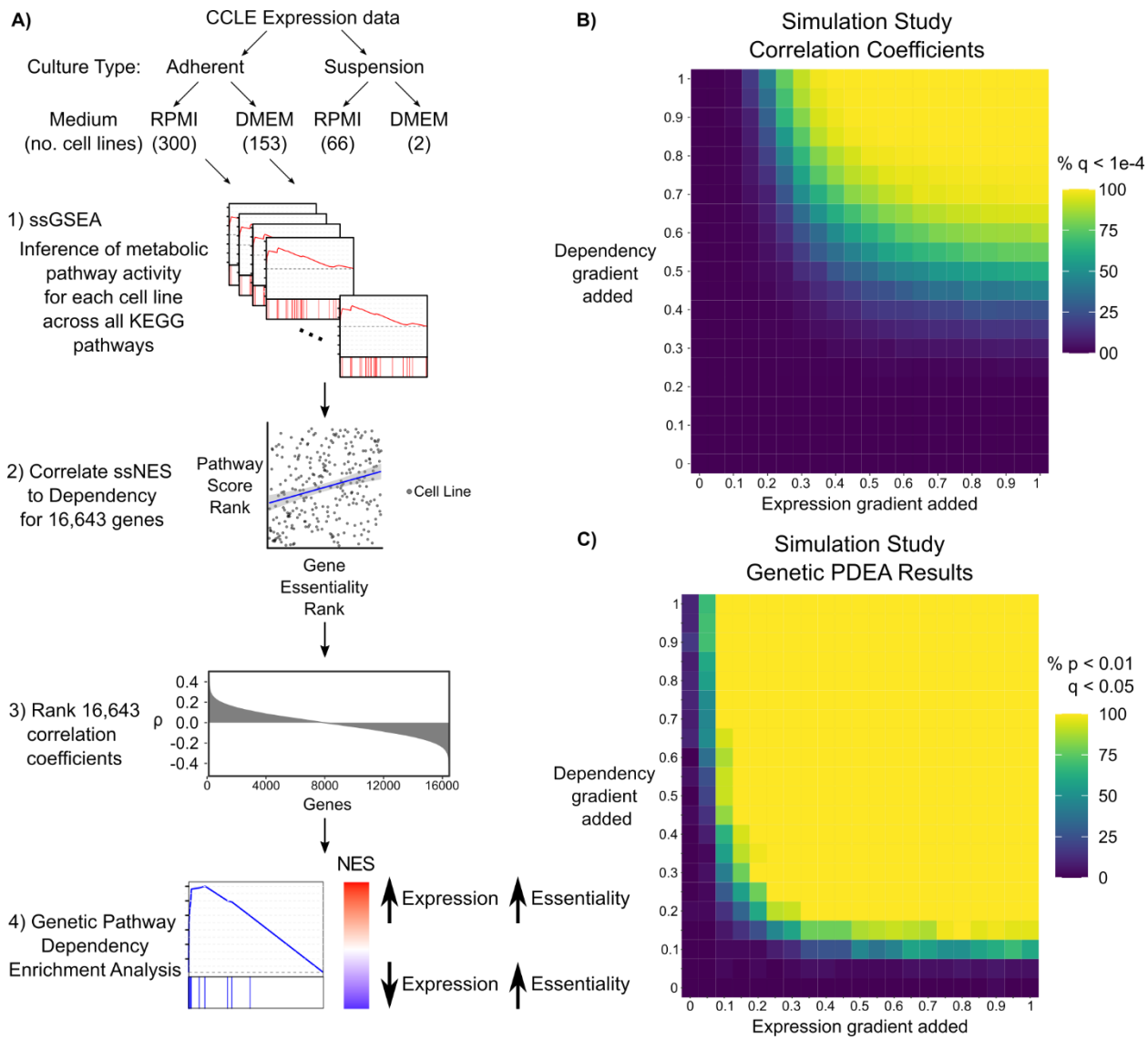

Figure 1. Integration of gene expression and CRISPR gene dependencies to identify metabolic pathway dependencies. A) Schematic outlining the approach for Genetic Pathway Dependency Enrichment Analysis (Genetic PDEA). Cancer cell lines from the CCLE were first stratified by culture type (adherent, suspension) and culture medium (RPMI, DMEM), and then their metabolic pathway activity was inferred using single-sample GSEA (ssGSEA). The resulting pathway activities were integrated with gene dependency to assess association with metabolic pathway activity. **B-C)** Simulated data (see methods) was used to assess the sensitivity of the Genetic PDEA approach. The heatmaps represent the percentage of significant results at each gradient added. Values added to the expression gradient resulted in slightly stronger correlation coefficients and Genetic PDEA results compared to values added to dependency gradient.

essentiality of the entire metabolic pathway, as opposed to individual genes, we then ranked the resulting 16,643 correlation coefficients and analyzed the rank list using GSEA again querying the KEGG metabolic pathways. Here, positive NES values represent increased pathway

dependency upon increased pathway activity, whereas negative NES values represent increased pathway dependency upon decreased pathway activity. Because this approach integrates the essentiality of all genes across a metabolic pathway into a single metric of pathway dependency, we termed this approach genetic pathway dependency enrichment analysis (Genetic PDEA).

To analyze the sensitivity of our Genetic PDEA approach, we analyzed simulated gene expression and gene dependency data using the pipeline outlined in Fig. 1A. Gene expression data (16,643 genes) was simulated for 300 cell lines using a normal distribution for each cell line ($\mu = 0$, $\sigma = 1$). Then, a synthetic gene set of 25 genes was perturbed using a normal distribution gradient. In cell line 1, the 25 genes were replaced with values from a normal distribution with $\mu = -X$, $\sigma = 1$, and in cell line 300, the 25 genes were replaced with values from a normal distribution with $\mu = +X$, $\sigma = 1$. For cell lines 2-299, the 25 genes were replaced with values from normal distributions with μ sequentially increasing from -X to X. ssGSEA NESs were then calculated for the synthetic gene set for all 300 cell lines. Next, gene dependency data was simulated for the same 300 cell lines using a similar normal distribution gradient method. For both gene expression and gene dependency data, values for the perturbation X were varied from 0 to 1. Then, Spearman correlation coefficients between synthetic gene set activity (ssGSEA NESs) and gene dependency were calculated for all 16,643 genes. Finally, GSEA was run to calculate the simulated Genetic PDEA values as outlined in Fig. 1A. Analyzing 50 replicates of this simulation pipeline, we found that both the correlation coefficients and Genetic PDEA NES results were more strongly influenced by expression gradients added than dependency gradients added (**Fig. 1B,C**). This suggests that our Genetic PDEA approach to identify metabolic pathway vulnerabilities in cancer cells is more sensitive to changes in metabolic pathway activity than changes in gene dependency. However, when the perturbation X was large for the dependency gradient and small

for the expression gradient (or vice versa), significant Genetic PDEA NES values were still obtained.

Having validated the sensitivity of our Genetic PDEA approach, we next investigated cancer cell line dependency across all KEGG metabolic pathways. We tested a total of 4,692 metabolic pathway combinations and identified 190 significant associations (FDR < 0.05) between metabolic pathway activity and pathway dependency in the adherent RPMI data set and an additional 190 significant associations in the adherent DMEM data set (**Supp. Table 1**). We next clustered Genetic PDEA NES values across all pathway activities (columns) and pathway dependencies (rows) (**Fig. 2A & Supp. Fig 1A**) and found that dependencies clustered together based on the function of the metabolic pathway activities more so than the function of the pathway dependency. For example, glycan biosynthesis pathways exhibit similar correlations with dependencies of other glycan pathways (columns) but differ in their own dependency (rows). We also found that the no single metabolic pathway had uniquely positive or negative NES values, suggesting that cancer cells are not universally dependent on any metabolic pathway. Interestingly, the strongest metabolic dependency of adherent RPMI cancer cell lines was Folate Biosynthesis (hsa00790) when One Carbon Pool by Folate (hsa00670) pathway activity was high (**Fig. 2B**). This enrichment was driven by the genes *QDPR*, *ALPI*, *ALPP*, and *GCH1*. Notably, Folate Biosynthesis is directly upstream of One Carbon Pool by Folate. Furthermore, one of the strongest Genetic PDEA results in both the adherent DMEM and adherent RPMI analyses recapitulated a link between increased dependency on One Carbon Pool by Folate in cells with increased TCA cycle activity (May et al., 2019) (**Fig. 2C & Supp. Fig. 1B**). Additionally, some metabolic pathways exhibited context-specific dependencies. For example, the dependency on the TCA Cycle (hsa00020) was increased in adherent RPMI cell lines with decreased Glycolysis-

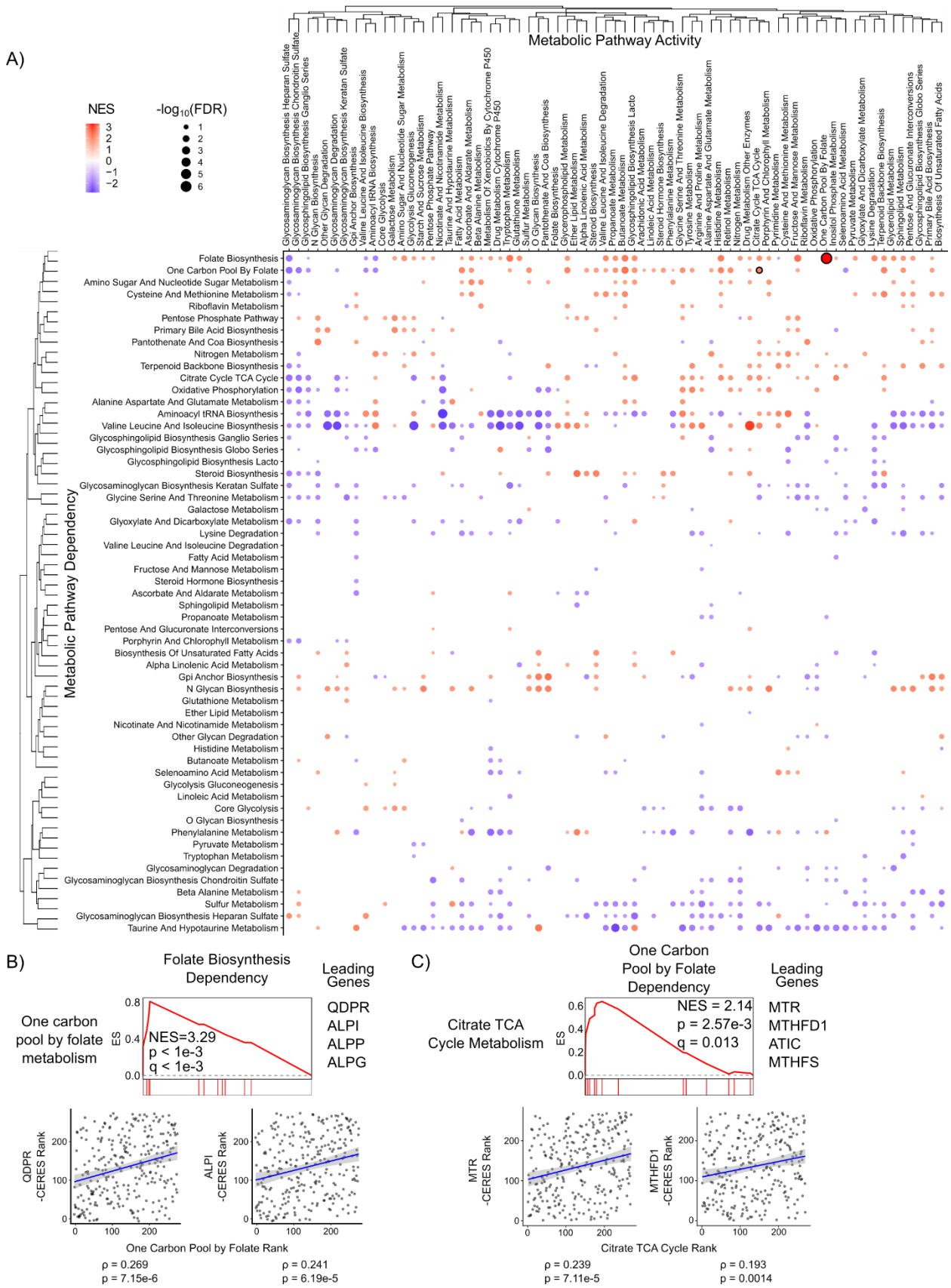
A)
Metabolic Pathway Activity
Metabolic Pathway Dependency
NES
-log10(FDR)
B)
Folate Biosynthesis Dependency
Leading Genes
One carbon pool by folate metabolism
NES=3.29
p < 1e-3
q < 1e-3
QDPR
ALPI
ALPP
ALPG
QDPR -CERES Rank
ALPI -CERES Rank
One Carbon Pool by Folate Rank
ρ = 0.269
p = 7.15e-6
ρ = 0.241
p = 6.19e-5
C)
One Carbon Pool by Folate Dependency
Leading Genes
Citrate TCA Cycle Metabolism
NES = 2.14
p = 2.57e-3
q = 0.013
MTR
MTHFD1
ATIC
MTHFS
MTR -CERES Rank
MTHFD1 -CERES Rank
Citrate TCA Cycle Rank
ρ = 0.239
p = 7.11e-5
ρ = 0.193
p = 0.0014

Figure 2. Global analysis of metabolic dependency data reveals context-specific pathway essentialities. A) Metabolic pathway activity was inferred using ssGSEA for 300 adherent cell lines cultured in RPMI and correlated to gene dependency data from The Cancer Dependency Map (DepMap). Correlation coefficients were then ranked and Genetic Pathway Dependency Enrichment Analysis (Genetic PDEA) was run using the KEGG metabolic pathways (see Fig. 1). Hierarchical clustering was performed on the Genetic PDEA normalized enrichment scores (NES). Results for pathways with FDR < 0.25 are plotted. Dots are colored according to their NES and sized according to the $-\log_{10}$ of the false discovery rate (FDR). Numerical values for each pathway can be found in Supp. Table 1. Results shown in B and C are highlighted with a black outline. **B)** Cancer cell dependency on Folate Biosynthesis (hsa00790) was increased when One Carbon Pool by Folate (hsa00670) pathway activity was high. The scatter plots of pathway activity NES and gene dependency (-CERES) for leading-edge genes *QDPR* and *ALPI* are shown**. C)** Dependency on One Carbon Pool by Folate metabolism (hsa00670) is increased when TCA cycle (hsa00020) activity is increased. The scatter plots of pathway activity NES and gene dependency (-CERES) for leading-edge genes *MTR* and *MTHFD1* are shown.

Gluconeogenesis (hsa00010) activity, whereas dependency on the TCA cycle was increased in adherent RPMI cell lines with increased Pentose Phosphate Pathway (hsa00030) activity (**Supp. Fig. 2**). This suggests that the diversion of glucose from glycolysis to the pentose phosphate pathway may confer increased dependency on the TCA Cycle. We next asked whether there existed a general relationship between a metabolic pathway's activity and its own essentiality. Of the 69 metabolic pathways queried, 36 had a negative NES and 33 had a positive NES for adherent RPMI cell lines (**Supp. Fig. 3A**). A similar distribution was observed in DMEM, although the pathways with positive and negative NES values were not the same as in RPMI (**Supp. Fig. 3B**). These results suggest that there is no generic rule regarding a metabolic pathway's activity and its essentiality. Rather, these results indicate that metabolic pathway dependency is highly context specific.

Media Composition Influences Metabolic Pathway Dependency

We next investigated whether cancer cell line metabolic pathway dependencies were influenced by media composition. To assess the essentiality of a pathway, we weighted each NES

Figure 3. Media composition influences metabolic pathway dependency. For adherent cancer cell lines cultured in RPMI (Fig. 2) and DMEM (Supp. Fig. 1A), the metabolic pathway dependency NESs from Genetic PDEA analysis were weighted by -$\log_{10}$ FDR. The weighted NESs were then averaged across all 69 KEGG metabolic pathways. Pathways are ranked by the difference between DMEM and RPMI. The relative media composition between RPMI and DMEM are shown on the right on a purple to green heat map with the relevant metabolite(s) indicated. For pathways with multiple metabolites, the average of the metabolites was taken. For example, the concentration of folate in RPMI and DMEM is 4 mg/L and 1 mg/L, respectively. The dependency on Folate Biosynthesis was much higher in DMEM than in RPMI because these cells must synthesize more folate. Conversely, the dependency on oxidative phosphorylation is much higher in DMEM. This may be due to differences in aspartate levels (RPMI 150 µM, DMEM 0 µM). The indicated pathways are highlighted in bold.

from Genetic PDEA by its -$\log_{10}$ FDR and then took the mean of all weighted NESs. We found striking differences between DMEM and RPMI metabolic pathway essentialities that can be partly explained by media composition (**Fig. 3**), consistent with the finding that the essentiality of individual metabolic genes is influenced by culture medium (Lagziel et al., 2019). For example, cancer cells cultured in RPMI exhibited a strongly positive average weighted NES for Folate Biosynthesis (hsa00790) whereas cancer cells cultured in DMEM did not. Notably, DMEM contains four times the concentration of folate (4 mg/L) compared to RPMI (1 mg/L), suggesting that cancer cells grown in DMEM need to synthesize less folate, thereby reducing their dependency on Folate Biosynthesis. Similarly, cancer cells grown in DMEM were more dependent on Oxidative Phosphorylation (hsa00190) than cancer cells grown in RPMI. One function of oxidative phosphorylation is to enable aspartate synthesis to accept electrons from the electron transport chain (Birsoy et al., 2015; Sullivan et al., 2015). Since RPMI and DMEM contain 150 µM and 0 µM aspartate, respectively, the increased dependency on oxidative phosphorylation in DMEM may reflect an increased need for aspartate synthesis. Taken together, these results suggest that media composition influences cancer cell line metabolic pathway dependency and that future studies of metabolic vulnerabilities should take media composition into consideration.

Metabolic pathway activity is correlated with anti-cancer drug sensitivity

We next sought to integrate metabolic pathway activity with large scale pharmacologic screens. We used the PRISM drug repurposing database (Corsello et al., 2020), which contains 1,448 compounds screened against 499 cell lines at 8 different doses. Once again, cell lines were separately processed by culture type and culture medium with a focus on adherent cell lines. Compounds measured in less than 150 cell lines were removed from the analysis, leaving 1,390 compounds. We then correlated drug response area-under-the-curve (AUC) with metabolic

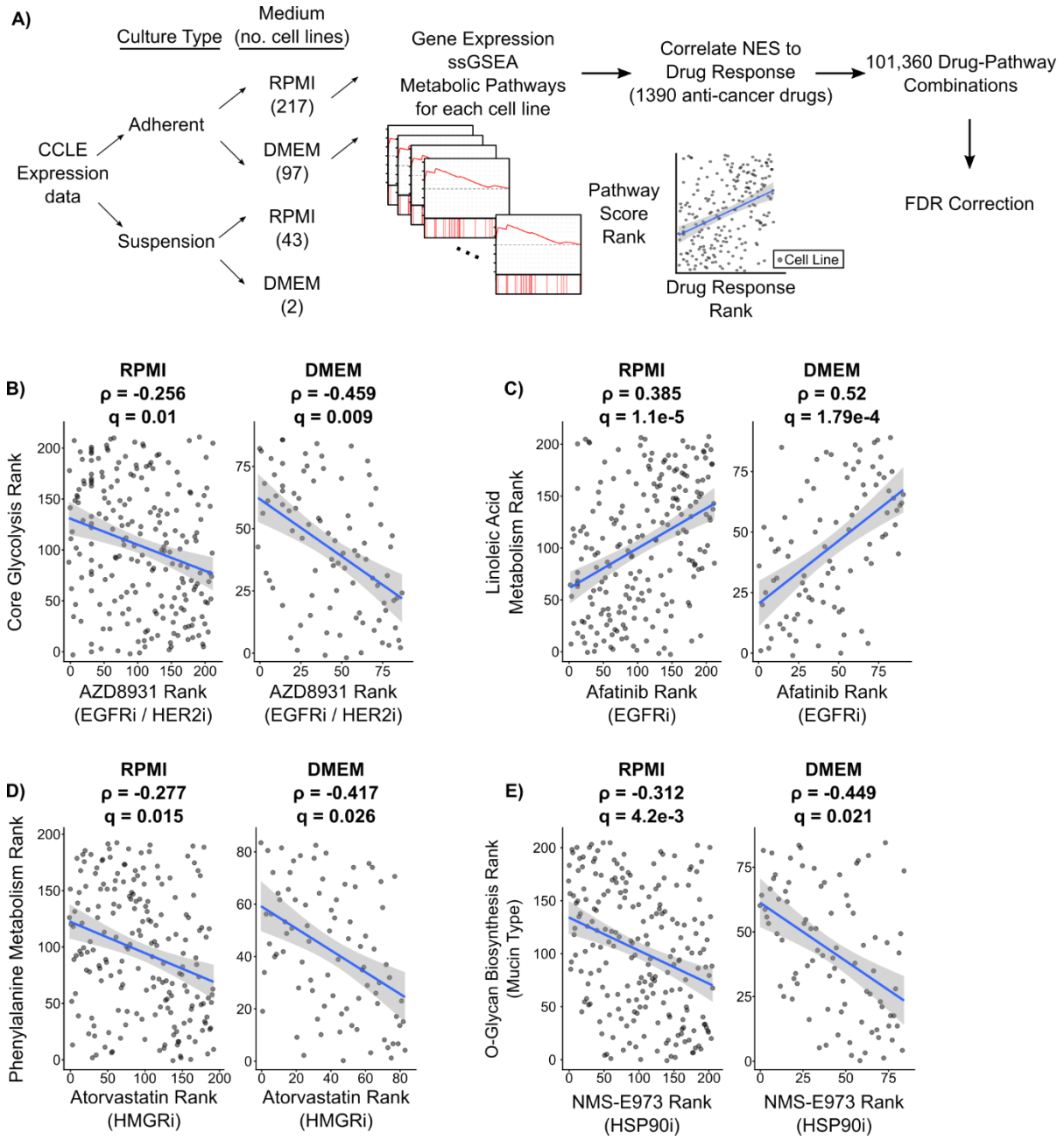

Figure 4. Metabolic pathway activity identifies anti-cancer drug sensitivity independent of cell culture medium. A) Schematic representing the strategy used to integrate metabolic pathway activity with drug response screens. Cancer cell lines were separately processed by culture type and culture medium with a focus on adherent cell lines. All correlation p-values were FDR corrected using a Benjamini-Hochberg correction. **B-E)** Scatter plots of significant drug:metabolic pathway combinations (FDR < 0.05) in both DMEM and RPMI mediums. Correlation coefficients and FDR corrected p-values are shown for each correlation. The annotated gene target of each drug is listed below the drug name. The remaining significant associations are listed in Supp. Table 2.

pathway activity after multiplying the response of drugs classified as positive regulators (e.g., agonists) by -1 for directional consistency (**Fig. 4A**). First, we asked whether there were any drugs with directional agreement across the RPMI and DMEM analyses. From a possible 101,360 possible drug:metabolic pathway combinations, 66 combinations passed FDR-corrected significance thresholds ($q < 0.05$) and were of the same sign in RPMI and DMEM (**Supp. Table 2**). Notably, zero results that passed FDR correction were of different sign. Many of the common associations in RPMI and DMEM were tyrosine kinase inhibitors (TKIs), which have been extensively linked to metabolism (Poliaková et al., 2018). Interestingly, we found a strong association between decreased Core Glycolysis (hsa_M00001) pathway activity and increased sensitivity to AZD8931, an inhibitor of EGFR and ERBB2 (HER2) (**Fig. 4B**). We also found a strong association between increased α-linoleic acid metabolism (hsa00592) and sensitivity to afatinib, another EGFR inhibitor (**Fig. 4C**). Of the non-TKI results, we found a link between decreased phenylalanine metabolism (hsa00360) and increased sensitivity to atorvastatin, an HMGR inhibitor (**Fig. 4D**). HMGR is the rate limiting enzyme in the cholesterol biosynthetic pathway (Burg and Espenshade, 2011) and multiple reports have suggested that elevated levels of phenylalanine inhibit cholesterol biosynthesis (Bhat and Ramasarma, 1979; Castillo et al., 1991; Shefer et al., 2000). Increased response to atorvastatin when phenylalanine metabolism activity is low suggests that decreased phenylalanine metabolism and HMGR inhibitors may be redundant. Lastly, we found a known link between decreased mucin type O-glycan biosynthesis pathway (hsa00512) activity and increased sensitivity to the HSP90 inhibitor NMS-E973 (Zhang et al., 2012) (**Fig. 4E**). Taken together, these results indicate that metabolic pathway activity can be associated anti-cancer drug sensitivity independent of cell culture medium.

Pharmacological Pathway Dependency Enrichment Analysis Reveals Common Metabolic Pathway Vulnerabilities

Having identified strong associations between metabolic pathway activity and individual drugs, we next asked whether there were commonalities in the response of cancer cell lines to families of metabolic pathway inhibitors. Drugs were mapped to metabolic pathways using their annotated target(s) and grouped according to the KEGG metabolic pathways database. Drugs were also classified as positive or negative regulators based on their annotated mechanism of action. For example, drugs labeled as “agonists” or “activators” were classified as positive regulators whereas “blockers” and “antagonists” were classified as negative regulators. To enable a consistent pathway analysis, correlation coefficients for positive regulators were multiplied by -1. Pathways with less than 4 drugs were omitted from the analysis, leaving 46 sets of drugs targeting metabolic pathways. We then analyzed the enrichment of these metabolic pathway inhibitors in the rank list of drug sensitivity-metabolic pathway activity correlation coefficients (n=1,390). We termed this approach Pharmacological Pathway Dependency Enrichment Analysis (Pharmacological PDEA) (**Supp. Fig. 4A**). To test the sensitivity of this approach, we again performed a simulation study with simulated gene expression data and simulated drug sensitivity (1,390 drugs). This approach was analogous to the simulation study of Figure 1B with 1,390 drug sensitivities replacing 16,643 gene dependencies. Similar to Genetic PDEA, we found that expression gradients resulted in stronger results than dependency gradients for both individual drug correlation coefficients and Pharmacological PDEA (**Supp. Fig. 4B-C**).

We then clustered the pharmacological PDEA NESs and found that pathways with similar function clustered together based on inhibitor dependencies (columns) more than with their dependency profile across pathways (rows) (**Fig. 5A and Supp. Fig. 5**), similar to our results with Genetic PDEA (**Fig. 2**). For example, the activities of Core Glycolysis (hsa_M00001), Fructose and Mannose Metabolism (hsa00051), Starch and Sucrose Metabolism (hsa00500), and Pentose

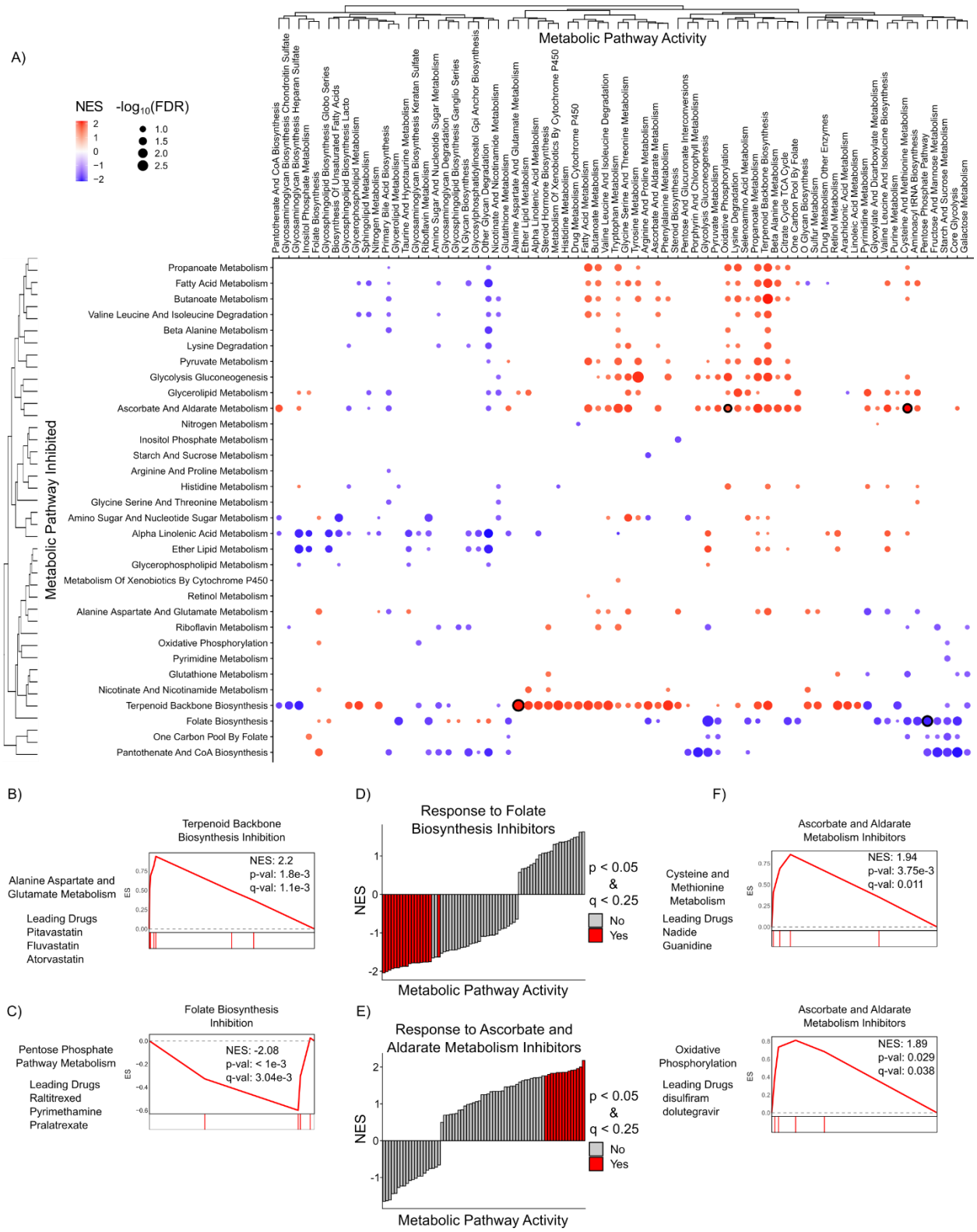

Figure 5. Pharmacological PDEA reveals consistent metabolic pathway vulnerabilities in Adherent RPMI cell lines. A) Pharmacological PDEA (Supp. Fig. 4) was performed on 1,390 anti-cancer drugs from the PRISM database. Drugs were mapped to metabolic pathways by their annotated target(s) and then the enrichment of these metabolic pathway inhibitors was analyzed

in the rank list of drug sensitivity-metabolic pathway activity correlation coefficients. Hierarchical clustering was performed on NES values, and results with FDR < 0.25 are plotted. Dots are colored according to the NES and sized according to the $-\log_{10}$ FDR. Dots with black outline correspond to results shown in panels B-C and F. **B-C)** Increased alanine, aspartate, and glutamate metabolism (hsa00250) correlates with increased response to inhibitors of terpenoid backbone biosynthesis. In contrast, decreased pentose phosphate pathway metabolism correlates with increased response to inhibitors of Folate Biosynthesis (hsa00790). **D-E)** Inhibitors of Folate Biosynthesis (hsa00790) are more effective when overall metabolic pathway expression is low, whereas inhibitors of Ascorbate and Aldarate Metabolism (hsa00053) are more effective when overall metabolic pathway expression is high. **F)** Representative mountain plots and the drug(s) driving enrichment of metabolic pathway activities that strongly correlate with response to inhibitors of Ascorbate and Aldarate metabolism are shown.

Phosphate Pathway (hsa00030) were clustered together in the adherent RPMI cell lines. Among the strongest Pharmacological PDEA results, we found that sensitivity to inhibitors of Terpenoid Backbone Biosynthesis (hsa00900) was increased in adherent RPMI cancer cells with high Alanine, Aspartate, and Glutamate Metabolism (hsa00250) (**Fig 5B**). We also found an interesting link between decreased pentose phosphate pathway (PPP) pathway activity and increased sensitivity to folate biosynthesis inhibitors (**Fig. 5C**). Because folate biosynthesis inhibitors prevent the generation of NADPH via one-carbon metabolism, these inhibitors may be more damaging to cellular redox balance when PPP expression is low. In fact, most strong results for inhibitors of folate biosynthesis occur when overall metabolic pathway activity is low (**Fig. 5D and Supp. Fig. 5B**). Conversely, inhibitors of Ascorbate and Aldarate metabolism (hsa00053) are more effective when overall metabolic pathway activity is high (**Fig. 5E**). This may be because ascorbate (also known as Vitamin C) is an effective antioxidant used to detoxify reactive oxygen species (ROS). ROS are a byproduct of many metabolic reactions such as oxidative phosphorylation and methionine metabolism, which indirectly produces ROS by supporting polyamine synthesis (Zhang et al., 2020). Indeed, the sensitivity to inhibitors of Ascorbate and Aldarate metabolism is stronger when expression of these ROS producing pathways is high (**Fig. 5F**) suggesting that ascorbate's role as an antioxidant is crucial in this context. Taken together,

these results reveal contexts in which pharmacological inhibition of metabolic pathways results in decreased cell survival.

Integration of pharmacologic and genetic screens reveals consistent metabolic vulnerabilities

Next, we sought to integrate results from genetic and pharmacological screen data to identify consistent metabolic pathway dependencies found independently in both analyses. First, we integrated individual gene dependency correlations with their corresponding drug sensitivity correlations by first annotating each drug with its gene target(s). We then summed the gene dependency correlation coefficient and the drug sensitivity correlation coefficient for each drug target and assessed significance by a permutation test with FDR correction (**Fig. 6A**). Out of 187,818 gene+drug:metabolic pathway combinations, we found 176 results that passed an FDR-corrected significance threshold of 0.01 (**Supp. Table 4**). Interestingly, all significant results targeted known cancer driver genes such as *EGFR*, *HER2*, *PIK3CA*, and *BRAF* (**Fig. 6B-E**). These results included a known interaction between HER2 inhibitors and retinol metabolism, whereby increased retinol metabolism enhances sensitivity to HER2 inhibition (Koay et al., 2010) (**Fig. 6C**). Additionally, some results identified well known molecular interactions, such as *BRAF* and *PIK3CA* driving sugar metabolism (Fruman et al., 2017; Parmenter et al., 2014) (**Fig. 6D,E**). These results demonstrate robust associations between metabolic pathway activity, gene dependency, and drug response.

Lastly, we sought to integrate the results from Genetic PDEA and Pharmacological PDEA to identify metabolic pathway vulnerabilities that were consistent between gene dependency and drug response data (**Fig. 6F**). By applying p-value and q-value filters to each analysis, we found

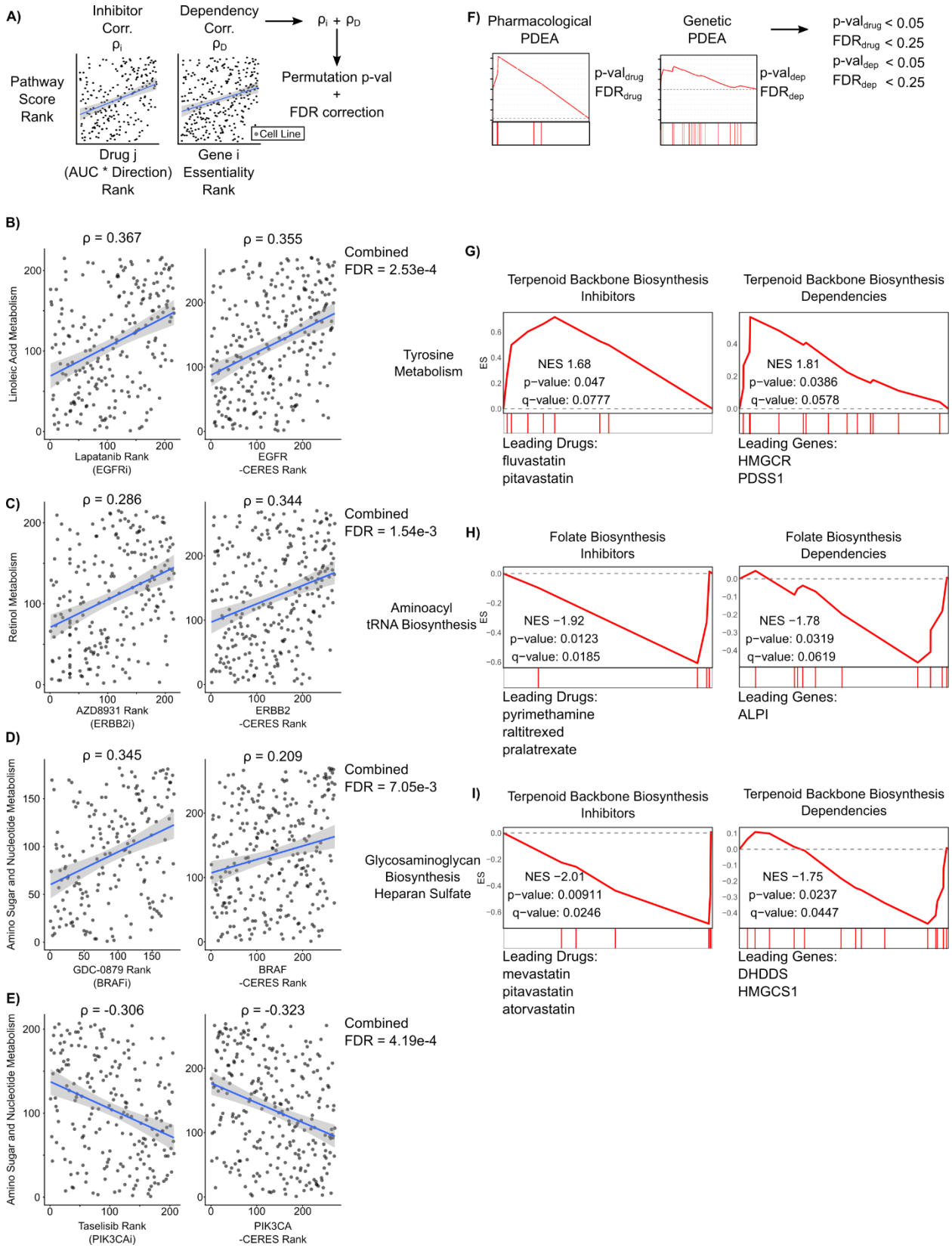

Figure 6. Integration of pharmacological and genetic screens reveals consistent metabolic pathway vulnerabilities in adherent RPMI cell lines. A) Schematic outlining approach to

identify drug targets and genetic dependencies that are commonly increased or decreased with metabolic pathway activity. Significance was assessed by permutation testing combined with Benjamini-Hochberg FDR correction. 176 significant associations of 187,818 gene+drug:metabolic pathway combinations passed the FDR threshold of 0.01 (Supp. Table 4). **B-E)** Scatter plots of four drug response and CRISPR gene dependencies associated with metabolic pathway activity. The gene target of each drug is listed below the drug name. **F)** Schematic outlining a filtering approach used to identify common pathway-level vulnerabilities in Genetic PDEA and Pharmacologic PDEA. **G-I)** Mountain plots and leading edge drugs and genes from the three common pathway vulnerabilities are shown.

three consistent vulnerabilities that were significant in both analyses. First, we found that when tyrosine metabolism is high, there is an increased vulnerability to inhibition or knockout of terpenoid backbone biosynthesis genes (**Fig. 6G**). Interestingly, the drugs driving the enrichment (fluvastatin and pitavastatin) target the protein with the largest gene dependency within the pathway, HMGCR. We also found a common vulnerability between inactivation of the folate biosynthesis pathway and decreased aminoacyl tRNA biosynthesis (**Fig. 6H**). Here, the top hits in Genetic PDEA and Pharmacological PDEA did not converge on a single protein product. Nevertheless, these results indicate that inactivation of the folate biosynthesis pathway is more effective at slowing cancer cell growth when aminoacyl tRNA biosynthesis pathway activity is low. Lastly, we found a strong association between inhibitors and gene knockouts of terpenoid backbone biosynthesis when pathway activity for biosynthesis of heparan sulfate is low (**Fig. 6I**). Once again, the targets of the statins driving the Pharmacological PDEA enrichment did not align with the top gene dependencies (*DHDDS*, *HMGCS1*). Taken together, these results demonstrate common metabolic pathway vulnerabilities by integrating gene dependency, drug response, and gene expression data.

Discussion

Traditionally, the analysis of gene essentiality in cancer cells has been limited to identification of individual genes required by cancer cells. Here, using metabolic pathways as an example, we have demonstrated an approach for identifying cancer cell dependencies at the level of pathways rather than individual genes. Illustrating the utility of our approach, we recapitulated known interactions between metabolic pathway activity, drug response, and gene dependency. These results build on a strong foundation of research identifying metabolic vulnerabilities in cancer cells (Lagziel et al., 2019; Luengo et al., 2017). Importantly, our results demonstrate that metabolic dependencies in cancer cells are highly context specific (**Fig. 2**) and are impacted by the nutritional microenvironment (**Fig. 3**). By investigating metabolic dependencies at the pathway level using genetic and pharmacological PDEA, we uncovered novel metabolic crosstalk, identified robust associations between drug response and metabolic pathway activity, and have discovered interactions between metabolic pathway activity and essentiality.

A recurring theme from our analyses is the importance of the pathways Folate Biosynthesis (hsa00790) and One Carbon Pool by Folate (hsa00670). Folate metabolism supports two key metabolic phenotypes commonly found in cancer cells by producing one carbon units for nucleotide synthesis and maintaining redox balance through production of NADPH (Locasale, 2013). In fact, two of the most widely used chemotherapeutics, methotrexate and 5-fluorouracil, target folate biosynthesis. In our analysis, we found that inhibitors of folate biosynthesis are highly effective when activity of other metabolic pathways is low (**Fig. 5D**). This may be because the drugs classified as folate biosynthesis inhibitors are anti-metabolites that cannot be metabolized by enzymes like thymidylate synthase or dihydrofolate reductase. When adjacent metabolic pathway expression is low, compensatory mechanisms cannot offset decreased folate biosynthesis, causing a crisis in both nucleotide synthesis and redox

homeostasis. Our results suggest that identifying biomarkers of activity for key pathways that control the sensitivity of antifolate pathways like the PPP (**Fig. 5C**) would enable advances in patient selection for antifolate chemotherapy.

The approach outlined here also sets the stage for the use of metabolic pathways to guide patient selection to therapy. Patient selection for targeted therapeutics such as EGFR inhibitors is often based on mutations and copy number alterations (CNAs), but even for these targeted therapeutics there exists a need to identify additional features that inform patient selection. Here, we identified metabolic pathways that strongly correlate with both CRISPR knockout and pharmacological inhibition of the oncogenes EGFR, HER2, BRAF, and PIK3CA (**Fig. 6**). This supports that metabolic pathways may be effective biomarkers even when mutations and CNAs in these oncogenes are not present (e.g., α-linoleic acid metabolism for sensitivity to EGFR inhibitors). Additionally, within patient populations with mutations or CNAs in these oncogenes, metabolic pathway activity could serve as a biomarker that predicts response to therapy. Furthermore, our results support that the statins targeting HMG-CoA reductase (*HMGCR*) might be effective cancer therapeutics in tumors with high tyrosine metabolism and/or low heparan sulfate glycosaminoglycan biosynthesis. Taken together, our results demonstrate that there may be patient benefit in analyzing tumor metabolism to inform patient selection for targeted therapies.

Our analysis identified media composition as a major confounding factor when analyzing cancer cell metabolic pathway dependencies (**Fig. 3**). This finding is consistent with recent studies and demonstrates the effect to which metabolism and metabolic vulnerabilities are shaped by the tumor microenvironment (Han et al., 2020; Lagziel et al., 2019). As such, our results highlight the importance of formulating cell culture mediums that better recapitulate the tumor

microenvironment (Cantor et al., 2017). Furthermore, the data used in this study comes from adherent cell lines cultured on tissue culture plastic. This removes environmental stresses such as concentration gradients and physical stimuli that cells experience in real tumors. Recent efforts have demonstrated that CRISPR-Cas9 screens can be performed in 3D organoids (Han et al., 2020). As this technology becomes more widely used, computational approaches such as ours can be applied to identify differences in metabolic pathway dependencies between 2D and 3D culture. Similarly, culture conditions that better reflect the physiological conditions of tumors will enhance the therapeutic relevance of our approach.

While our study identified robust associations between drug response and metabolic pathway expression, these analyses (**Figs. 5 and 6**) rely on the annotated targets of these drugs. Off-target toxicity is a major concern when using small molecule inhibitors. In fact, some recent studies have found that off-target toxicity drives the anti-tumor effect of these compounds (Lin et al., 2019). As such, we cannot exclude the possibility that off-target effects of these compounds could cause the associations identified here. Furthermore, some compounds in this study are quite promiscuous with multiple annotated protein targets. This promiscuity confounds the Pharmacologic PDEA analysis (**Fig. 5**) since some drugs were mapped to multiple metabolic pathways. As such, the utility of the Pharmacologic PDEA approach lies in the aggregation of multiple drugs to arrive at a conclusion, rather than treating each individual drug as significant. In addition, by integrating the Pharmacologic PDEA and Genetic PDEA results (**Fig. 6**), we strengthened our confidence in the association between metabolic pathway activity and pathway dependency.

Another potential weakness of our study is that we rely on the inference of metabolic pathway activity from gene expression data. Gene expression, however, does not always accurately reflect cellular metabolism. First, proteomic studies have shown that protein expression does not always correlate with gene expression (Liu et al., 2016). Second, metabolic enzyme activity can be regulated by post translational modifications (Brunk et al., 2018; Oliveira et al., 2012). By using gene expression data, we have not accounted for these factors, and as such our analysis may not reflect pathway activity at the metabolic flux level. We expect that expanding recent efforts to characterize metabolite abundance (Li et al., 2019) and metabolite flux (Chen et al., 2019) in panels of cancer cell lines will improve our ability to identify metabolic pathway vulnerabilities by providing better measures of metabolic pathway activity.

Taken together, this study serves as a comprehensive characterization of the landscape of metabolic pathway vulnerabilities. Furthermore, our approach serves as a framework for integrating gene expression, gene dependency, and drug response data to uncover metabolic dependencies at the level of pathways rather than individual genes. We anticipate this approach could be extended to other biologically relevant pathways beyond metabolism. Furthermore, the utility of our approach will increase as CRISPR-Cas9 and pharmacologic screening expand to include more cancer cell lines, better measure of cellular metabolism, and physiologically relevant models like 3D organoids.

Methods

Data Sources

Cancer cell line gene expression data was downloaded from the Cancer Cell Line Encyclopedia (CCLE) version 19Q4. Gene dependency data was downloaded from the Cancer Dependency Map (DepMap), Achilles gene effect version 19Q4 was used for this study. Drug response data was downloaded from the PRISM Repurposing database, version 19Q4 with secondary screen with dose response curve parameters was used. Metabolic pathway annotations were downloaded from the Kyoto Encyclopedia of Genes and Genomes (KEGG).

Simulation Studies

Gene expression data was simulated for 300 cell lines using a normal distribution for each cell line ($\mu = 0$, $\sigma = 1$). Then, a synthetic gene set of 25 genes was perturbed using a normal distribution gradient, where cell line 1 received a value randomly selected from a normal distribution with $\mu = -X$, $\sigma = 1$ and cell line 300 received a value randomly selected from a normal distribution of $\mu = +X$, $\sigma = 1$, with cell lines 2-299 receiving values randomly selected from normal distributions with sequentially increasing values μ from -X to X. Single-sample Gene Set Enrichment Analysis (ssGSEA) was calculated for the synthetic gene set for all 300 cell lines. Next, gene dependency data was simulated for the same 300 cell lines using the same normal distribution gradient method. For both gene expression and gene dependency data, values for X were varied from 0 to 1. Next, Spearman correlation coefficients between synthetic gene set activity (NES) and gene dependency were calculated for all 16,643 genes. Finally, Gene Set Enrichment Analysis was run to calculate the simulated Genetic Pathway Dependency Enrichment Analysis values. For the Pharmacological PDEA simulation study in Supp. Figure 4, a similar approach was used with 200 cell lines and 1,390 drugs to simulate the data used in the Pharmacological PDEA study.

Calculation of Metabolic Pathway Expression

1,019 cancer cell lines from the CCLE were separated by their culture type (adherent or suspension) and then culture medium (RPMI or DMEM), respectively. Cell lines with missing information for either culture type or medium were omitted. Gene expression values were unit normalized across all cell lines of the same culture and medium type (e.g. Adherent RPMI). Single-sample Gene Set Enrichment Analysis (ssGSEA) across all metabolic pathways in the KEGG database was run on the normalized gene expression values, giving normalized enrichment scores (NES) representing relative metabolic pathway activity for 69 metabolic pathways for each cell line.

Genetic Pathway Dependency Enrichment Analysis

For each metabolic pathway, the NES was correlated with the -CERES score for all 16,643 genes. Due to the bimodal nature of NESs, Spearman correlations were used. The resulting correlation coefficients were ranked and GSEA querying KEGG metabolic pathways was run to calculate Genetic Pathway Dependency Enrichment Analysis (Genetic PDEA). Positive NES represent increased essentiality upon increased metabolic pathway activity, whereas negative NES represent increased essentiality upon decreased metabolic pathway activity.

Drug Response Correlations

For each metabolic pathway, the NES was correlated with the -AUC (area under the curve) for 1,448 anti-cancer drugs in the PRISM repurposing database. Drugs with less than 150 cell lines were removed, leaving 1,390 drugs. Spearman correlation p-values were calculated and a Benjamini-Hochberg false discovery rate correction was applied for each metabolic pathway.

Pharmacological Pathway Dependency Enrichment Analysis

Drugs were mapped to their metabolic pathway using the annotated target(s) and genes from KEGG metabolic pathways. Since the PRISM database contains both activators and inhibitors, we annotated all activators by mechanism of action and multiplied their correlation coefficients by -1. Therefore, a pathway activator would be counted similarly to a pathway inhibitor. Pathways with 4 or more drugs were kept. Then, GSEA was run on the rank lists of 1390 correlation coefficients.

Integration of Individual Drug Response and Gene Dependency

Drug-gene dependency pairs were mapped using the target annotations for each drug. Correlation coefficients for each drug and gene dependency were summed for each metabolic pathway, generating 187,818 drug+gene:pathway combinations. An empirical permutation test was run sampling 1,000 combinations of each drug+gene correlation coefficient. P-values were calculated by dividing the number of permutations that out-performed the real summed correlation coefficients by the number of same-signed permutations. P-values were then adjusted using a Benjamini-Hochberg correction for each metabolic pathway.

Integration of Genetic PDEA and Pharmacological PDEA

Results from Genetic PDEA and Pharmacological PDEA were filtered for same signed NES and p-values of less than 0.05 and FDR values of less than 0.25 (per the original GSEA algorithm). Three pathway-drug-gene dependencies were identified out of a possible 3,220 combinations.

Code Availability

Our code is freely available for use at: https://github.com/JamesJoly/MetabolicDependencies

Acknowledgments

This work was supported by the American Cancer Society Grant IRG-16-181-57, the 2020 AACR-Bayer Innovation and Discovery Grant, Grant Number 20-80-44-GRAH, and the Viterbi School of Engineering.

Conflict of Interest Statement

The authors declare no conflicts of interest.

Author Contributions

JHJ conceived the project. JHJ and BTLC performed research. JHJ and NAG analyzed data. JHJ and NAG wrote the manuscript.

References

Barbie, D.A., Tamayo, P., Boehm, J.S., Kim, S.Y., Moody, S.E., Dunn, I.F., Schinzel, A.C., Sandy, P., Meylan, E., Scholl, C., et al. (2009). Systematic RNA interference reveals that oncogenic KRAS-driven cancers require TBK1. Nature *462*, 108–112.

Barretina, J., Caponigro, G., Stransky, N., Venkatesan, K., Margolin, A.A., Kim, S., Wilson, C.J., Lehár, J., Kryukov, G.V., Sonkin, D., et al. (2012). The Cancer Cell Line Encyclopedia enables predictive modelling of anticancer drug sensitivity. Nature *483*, 603–607.

Bhat, C.S., and Ramasarma, T. (1979). Effect of Phenyl and Phenolic Acids on Mevalonate-5-Phosphate Kinase and Mevalonate-5-Pyrophosphate Decarboxylase of the Rat Brain. Journal of Neurochemistry *32*, 1531–1537.

Birsoy, K., Wang, T., Chen, W.W., Freinkman, E., Abu-Remaileh, M., and Sabatini, D.M. (2015). An Essential Role of the Mitochondrial Electron Transport Chain in Cell Proliferation Is to Enable Aspartate Synthesis. Cell *162*, 540–551.

Brunk, E., Chang, R.L., Xia, J., Hefzi, H., Yurkovich, J.T., Kim, D., Buckmiller, E., Wang, H.H., Cho, B.-K., Yang, C., et al. (2018). Characterizing posttranslational modifications in prokaryotic metabolism using a multiscale workflow. PNAS *115*, 11096–11101.

Burg, J.S., and Espenshade, P.J. (2011). Regulation of HMG-CoA reductase in mammals and yeast. Prog Lipid Res *50*, 403–410.

Cantor, J.R., Abu-Remaileh, M., Kanarek, N., Freinkman, E., Gao, X., Louissaint, A., Lewis, C.A., and Sabatini, D.M. (2017). Physiologic Medium Rewires Cellular Metabolism and Reveals Uric Acid as an Endogenous Inhibitor of UMP Synthase. Cell *169*, 258-272.e17.

Castillo, M., Martínez-Cayuela, M., Zafra, M.F., and García-Peregrín, E. (1991). Effect of phenylalanine derivatives on the main regulatory enzymes of hepatic cholesterogenesis. Molecular and Cellular Biochemistry.

Chen, P.-H., Cai, L., Huffman, K., Yang, C., Kim, J., Faubert, B., Boroughs, L., Ko, B., Sudderth, J., McMillan, E.A., et al. (2019). Metabolic Diversity in Human Non-Small Cell Lung Cancer Cells. Mol. Cell *76*, 838-851.e5.

Corsello, S.M., Nagari, R.T., Spangler, R.D., Rossen, J., Kocak, M., Bryan, J.G., Humeidi, R., Peck, D., Wu, X., Tang, A.A., et al. (2020). Discovering the anticancer potential of non-oncology drugs by systematic viability profiling. Nat Cancer 1–14.

Dang, L., White, D.W., Gross, S., Bennett, B.D., Bittinger, M.A., Driggers, E.M., Fantin, V.R., Jang, H.G., Jin, S., Keenan, M.C., et al. (2009). Cancer-associated IDH1 mutations produce 2-hydroxyglutarate. Nature *462*, 739–744.

Deans, R.M., Morgens, D.W., Ökesli, A., Pillay, S., Horlbeck, M.A., Kampmann, M., Gilbert, L.A., Li, A., Mateo, R., Smith, M., et al. (2016). Parallel shRNA and CRISPR-Cas9 screens enable antiviral drug target identification. Nature Chemical Biology *12*, 361–366.

Fruman, D.A., Chiu, H., Hopkins, B.D., Bagrodia, S., Cantley, L.C., and Abraham, R.T. (2017). The PI3K Pathway in Human Disease. Cell *170*, 605–635.

Garnett, M.J., Edelman, E.J., Heidorn, S.J., Greenman, C.D., Dastur, A., Lau, K.W., Greninger, P., Thompson, I.R., Luo, X., Soares, J., et al. (2012). Systematic identification of genomic markers of drug sensitivity in cancer cells. Nature *483*, 570–575.

Ghandi, M., Huang, F.W., Jané-Valbuena, J., Kryukov, G.V., Lo, C.C., McDonald, E.R., Barretina, J., Gelfand, E.T., Bielski, C.M., Li, H., et al. (2019). Next-generation characterization of the Cancer Cell Line Encyclopedia. Nature *569*, 503–508.

Gonçalves, E., Segura-Cabrera, A., Pacini, C., Picco, G., Behan, F.M., Jaaks, P., Coker, E.A., van der Meer, D., Barthorpe, A., Lightfoot, H., et al. (2020). Drug mechanism-of-action discovery through the integration of pharmacological and CRISPR screens. Molecular Systems Biology *16*, e9405.

Graham, N.A., Minasyan, A., Lomova, A., Cass, A., Balanis, N.G., Friedman, M., Chan, S., Zhao, S., Delgado, A., Go, J., et al. (2017). Recurrent patterns of DNA copy number alterations in tumors reflect metabolic selection pressures. Molecular Systems Biology *13*, 914.

Han, K., Pierce, S.E., Li, A., Spees, K., Anderson, G.R., Seoane, J.A., Lo, Y.-H., Dubreuil, M., Olivas, M., Kamber, R.A., et al. (2020). CRISPR screens in cancer spheroids identify 3D growth-specific vulnerabilities. Nature 1–6.

Kanehisa, M., Goto, S., Sato, Y., Kawashima, M., Furumichi, M., and Tanabe, M. (2014). Data, information, knowledge and principle: back to metabolism in KEGG. Nucl. Acids Res. *42*, D199–D205.

Koay, D.C., Zerillo, C., Narayan, M., Harris, L.N., and DiGiovanna, M.P. (2010). Anti-tumor effects of retinoids combined with trastuzumab or tamoxifen in breast cancer cells: induction of apoptosis by retinoid/trastuzumab combinations. Breast Cancer Research *12*, R62.

Lagziel, S., Lee, W.D., and Shlomi, T. (2019). Inferring cancer dependencies on metabolic genes from large-scale genetic screens. BMC Biology *17*, 37.

Li, H., Ning, S., Ghandi, M., Kryukov, G.V., Gopal, S., Deik, A., Souza, A., Pierce, K., Keskula, P., Hernandez, D., et al. (2019). The landscape of cancer cell line metabolism. Nature Medicine *25*, 850–860.

Lin, A., Giuliano, C.J., Palladino, A., John, K.M., Abramowicz, C., Yuan, M.L., Sausville, E.L., Lukow, D.A., Liu, L., Chait, A.R., et al. (2019). Off-target toxicity is a common mechanism of action of cancer drugs undergoing clinical trials. Science Translational Medicine *11*.

Liu, Y., Beyer, A., and Aebersold, R. (2016). On the Dependency of Cellular Protein Levels on mRNA Abundance. Cell *165*, 535–550.

Locasale, J.W. (2013). Serine, glycine and one-carbon units: cancer metabolism in full circle. Nature Reviews Cancer *13*, 572–583.

Luengo, A., Gui, D.Y., and Vander Heiden, M.G. (2017). Targeting Metabolism for Cancer Therapy. Cell Chem Biol *24*, 1161–1180.

Maddocks, O.D.K., Berkers, C.R., Mason, S.M., Zheng, L., Blyth, K., Gottlieb, E., and Vousden, K.H. (2013). Serine starvation induces stress and p53-dependent metabolic remodelling in cancer cells. Nature *493*, 542–546.

May, J.L., Kouri, F.M., Hurley, L.A., Liu, J., Tommasini-Ghelfi, S., Ji, Y., Gao, P., Calvert, A.E., Lee, A., Chandel, N.S., et al. (2019). IDH3α regulates one-carbon metabolism in glioblastoma. Science Advances *5*, eaat0456.

Meyers, R.M., Bryan, J.G., McFarland, J.M., Weir, B.A., Sizemore, A.E., Xu, H., Dharia, N.V., Montgomery, P.G., Cowley, G.S., Pantel, S., et al. (2017). Computational correction of copy number effect improves specificity of CRISPR–Cas9 essentiality screens in cancer cells. Nature Genetics *49*, 1779–1784.

Muller, F.L., Colla, S., Aquilanti, E., Manzo, V.E., Genovese, G., Lee, J., Eisenson, D., Narurkar, R., Deng, P., Nezi, L., et al. (2012). Passenger deletions generate therapeutic vulnerabilities in cancer. Nature *488*, 337–342.

Oliveira, A.P., Ludwig, C., Picotti, P., Kogadeeva, M., Aebersold, R., and Sauer, U. (2012). Regulation of yeast central metabolism by enzyme phosphorylation. Mol Syst Biol *8*, 623.

Parmenter, T.J., Kleinschmidt, M., Kinross, K.M., Bond, S.T., Li, J., Kaadige, M.R., Rao, A., Sheppard, K.E., Hugo, W., Pupo, G.M., et al. (2014). Response of BRAF-Mutant Melanoma to BRAF Inhibition Is Mediated by a Network of Transcriptional Regulators of Glycolysis. Cancer Discov *4*, 423–433.

Poliaková, M., Aebersold, D.M., Zimmer, Y., and Medová, M. (2018). The relevance of tyrosine kinase inhibitors for global metabolic pathways in cancer. Mol Cancer *17*.

Sharma, A.K., Eils, R., and König, R. (2016). Copy Number Alterations in Enzyme-Coding and Cancer-Causing Genes Reprogram Tumor Metabolism. Cancer Res. *76*, 4058–4067.

Shefer, S., Tint, G.S., Jean-Guillaume, D., Daikhin, E., Kendler, A., Nguyen, L.B., Yudkoff, M., and Dyer, C.A. (2000). Is there a relationship between 3-hydroxy-3-methylglutaryl coenzyme a reductase activity and forebrain pathology in the PKU mouse? J. Neurosci. Res. *61*, 549–563.

Subramanian, A., Narayan, R., Corsello, S.M., Peck, D.D., Natoli, T.E., Lu, X., Gould, J., Davis, J.F., Tubelli, A.A., Asiedu, J.K., et al. (2017). A Next Generation Connectivity Map: L1000 Platform and the First 1,000,000 Profiles. Cell *171*, 1437-1452.e17.

Sullivan, L.B., Gui, D.Y., Hosios, A.M., Bush, L.N., Freinkman, E., and Vander Heiden, M.G. (2015). Supporting Aspartate Biosynthesis Is an Essential Function of Respiration in Proliferating Cells. Cell *162*, 552–563.

Tsherniak, A., Vazquez, F., Montgomery, P.G., Weir, B.A., Kryukov, G., Cowley, G.S., Gill, S., Harrington, W.F., Pantel, S., Krill-Burger, J.M., et al. (2017). Defining a Cancer Dependency Map. Cell *170*, 564-576.e16.

Wang, T., Yu, H., Hughes, N.W., Liu, B., Kendirli, A., Klein, K., Chen, W.W., Lander, E.S., and Sabatini, D.M. (2017). Gene Essentiality Profiling Reveals Gene Networks and Synthetic Lethal Interactions with Oncogenic Ras. Cell *168*, 890-903.e15.

Warburg, O. (1956). On the Origin of Cancer Cells. Science *123*, 309–314.

Ward, P.S., Patel, J., Wise, D.R., Abdel-Wahab, O., Bennett, B.D., Coller, H.A., Cross, J.R., Fantin, V.R., Hedvat, C.V., Perl, A.E., et al. (2010). The Common Feature of Leukemia-Associated IDH1 and IDH2 Mutations Is a Neomorphic Enzyme Activity Converting α-Ketoglutarate to 2-Hydroxyglutarate. Cancer Cell *17*, 225–234.

Zhang, F., Snead, C.M., and Catravas, J.D. (2012). Hsp90 regulates O-linked β-N-acetylglucosamine transferase: a novel mechanism of modulation of protein O-linked β-N-acetylglucosamine modification in endothelial cells. Am J Physiol Cell Physiol *302*, C1786–C1796.

Zhang, T., Bauer, C., Newman, A.C., Uribe, A.H., Athineos, D., Blyth, K., and Maddocks, O.D.K. (2020). Polyamine pathway activity promotes cysteine essentiality in cancer cells. Nature Metabolism 1–15.